DESIGN AND DEVELOPMENT FOR THE NEXT GENERATION X-RAY BEAM POSITION MONITOR SYSTEM AT THE APS*

B.X. Yang[#], G. Decker, S. H. Lee, Y. Jaski, F. Westferro, N. Sereno, and M. Ramanathan
Advanced Photon Source, Argonne National Laboratory, Argonne, IL 60439, USA

Abstract

The planned Advanced Photon Source (APS) Upgrade will bring storage ring beam sizes down to several micrometers and require x-ray beam directional stability in 100 nrad range for undulator power exceeding 20 kW. The next generation x-ray beam position monitors (XBPMs) are designed to meet these requirements. We present commissioning data on the recently installed grazing-incidence insertion device x-ray beam position monitor (GRID-XBPM) based on Cu K-edge x-ray fluorescence from limiting absorbers of the front end for two inline undulators. It demonstrated a 30-fold improvement for signal-to-background ratio over existing photoemission-based XBPMs. Techniques and results for calibrating the XBPMs are also discussed.

INTRODUCTION

The planned APS Upgrade (APS-U) will dramatically reduce the electron beam size and divergence in the horizontal plane [1]. A major improvement in beam stability is required for APS users to benefit from this upgrade. Table 1 lists the stability goals, which are approximately 10% of the expected beam sizes. A new FPGA-based orbit feedback system and several new diagnostics are being developed to support this goal [2]. Among them, a new class of x-ray beam position monitors (XBPM) sensitive to only hard x-ray excitations is being developed. For the high heat load front end in the APS-U, two inline undulators will deliver up to 20 kW of x-ray power. We developed a grazing-incidence XBPM (GRID-XBPM) using the Cu K-edge x-ray fluorescence (XRF) from the front-end apertures to infer the undulator beam's core position [3]. A prototype test showed a significant reduction in bend magnet (BM) background [4]. Following this successful demonstration, two GRID-XBPMs were designed and constructed in the new front end and installed in 2014 [5]. In this work, we report the commissioning results of the first production XBPM and present its performance in a front end.

Table 1: MBA Upgrade Beam Stability Requirements

	AC rms Motion (0.01-1000 Hz)	Long-term Drift (100 s - 7 Days)
Horizontal	1.7 μm / 0.25 μrad	1.0 μm / 0.6 μrad
Vertical	0.4 μm / 0.17 μrad	1.0 μm / 0.5 μrad

BEND MAGNET BACKGROUND

In a previous test [5], the prototype XBPM was located downstream of a 4.5-mm front end exit aperture, with a 0.2 mrad horizontal acceptance angle. In the front end, however, the XBPM is located at 18.6 m from the source, downstream of a 10.6-mm aperture, with a 0.6-mrad horizontal acceptance angle. The increase in horizontal aperture is expected to increase BM background. Therefore, characterizing its impact became our first task. We measured the sum signal of all diodes / blades with the undulator gap fully open and then as a function of undulator gaps. Figure 1 shows the ratio of the undulator signal over the BM background for the best group of PIN diodes in the GRID-XBPM, along with those for installed APS photoemission XBPMs. We can see that the hard x-ray XBPM improves the signal-to-background ratio by 30 fold. To further reduce the impact of the BM background, we built three groups of PIN diodes into the GRID-XBPM. Not surprisingly, while the "best" group is most sensitive to the photons originated near the undulator axis, the "worst" group of PIN diodes is located furthest away from the undulator axis and is more sensitive to the BM background by a factor of eight. Subtracting a small fraction of the "worst" PIN signals from the "best" PIN signals will further reduce the impact of BM background by another factor of 5. This requires a special 6-channel XBPM electronics. In the remaining part of this work, however, we will continue with the conventional 4-channel electronics for presenting our commissioning experience.
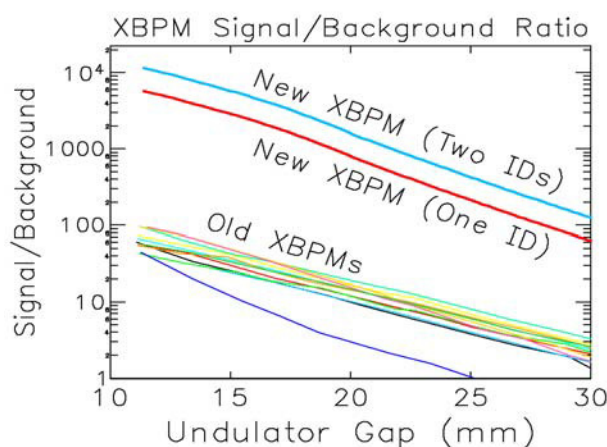

Figure 1: Ratio of undulator signal over BM background for the hard x-ray GRID-XBPM shows a 30-fold improvement over old style photoemission XBPMs.

VERTICAL CALIBRATION

The XBPM reads out vertical positions using x-ray pinhole camera optics [3]. Ideally the calibration factor is determined by the detector geometry and is independent of undulator gaps. To validate this design goal, we scanned the electron beam angle in the vertical plane with undulator gaps set between 11 and 30 mm, the range of interest to most APS users. The upper panel of Fig. 2 shows the calibration factor as a function of gaps, where US and DS are for upstream and downstream undulators, respectively. We can see that the variation of slopes are less than ±3% over the entire range of gaps of interest. Furthermore, Sector 27 used 33-mm-period undulators in 2014 and then upgraded to 27-mm-period undulators in 2015. The lower panel of Figure 2 shows the calibration constants measured in both undulators at 11-mm gap, with total variations less than ±1%. For possible offset of 100 μm from the BPM electric center, these variations may result in a beam position error under 3 μm, or beam angle error less than 0.16 mrad, well within the DC specifications in Table 1.
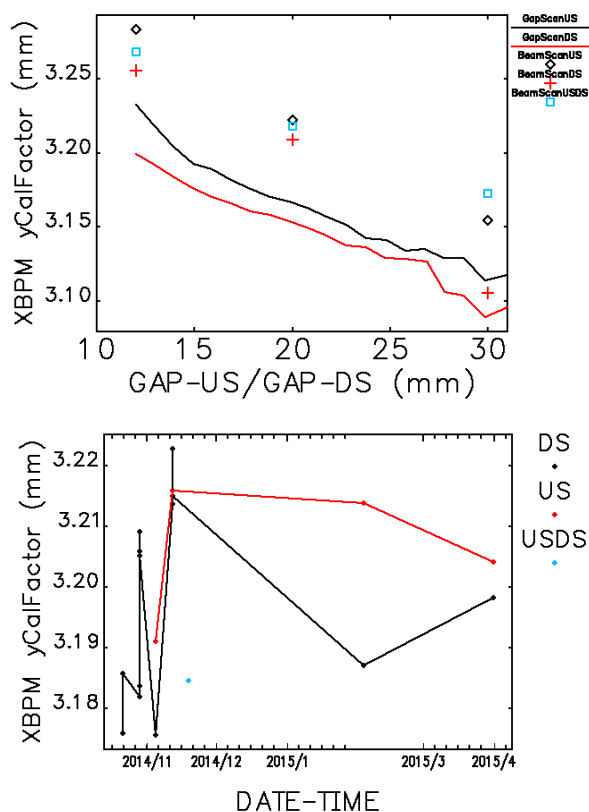

Figure 2: Upper panel: Calibration data for different undulator gap values demonstrates insensitivity to gaps. Lower panel: S27 GRID-XBPM calibration constants in 2014-2015 with different undulator configurations.

HORIZONTAL CALIBRATION

The XBPM derives horizontal beam position from the difference / sum of the x-ray detector signals from the left and right absorbers using the conventional expression,

$$x = k_x \frac{\Delta_x}{\Sigma_x} - x_0, \tag{1}$$

where the difference Δ_x and sum Σ_x are calculated from the diode signals A, B, C, and D. Since the horizontal XRF foot-print changes dramatically from the minimum gap (11 mm) to the maximum gap (30 mm), the calibration constants are strongly dependent on the gap. The upper panel of Fig. 3 shows the ratios Δ_x/Σ_x as functions of the projected electron beam position, which are straight lines within ±200 μm from the XBPM's electrical center. The lower panel of the figure plots the XBPM's sensitivity $(1/k_x)$ as a function of inverse undulator gap $(1/G)$. We found the curve to be straight lines between the gap values where one of the undulator harmonics coincides with the Cu K-edge. This piece-wise linear behavior can be used to interpolate XBPM calibration constant during user operations.
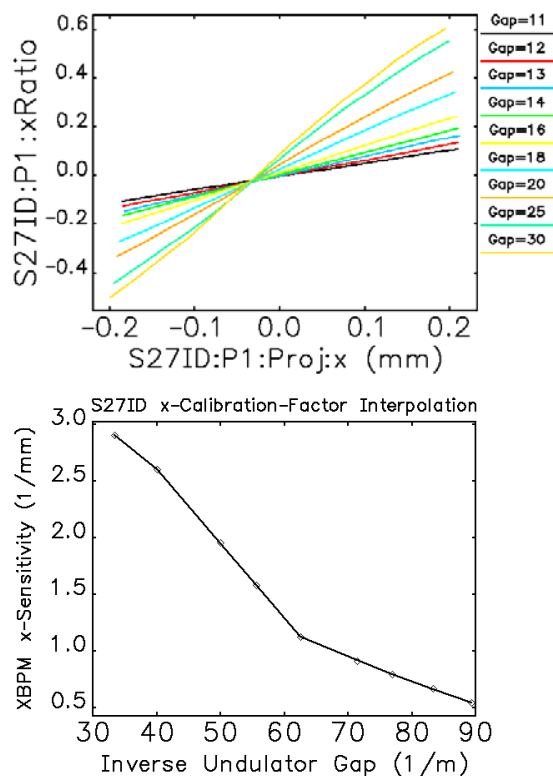

Figure 3: Upper panel: Horizontal XBPM calibration scan data. Lower panel: Horizontal XBPM sensitivity is a piece-wise linear function of inverse undulator gap.

ERROR CORRECTION

After the vertical and horizontal calibration factors are determined, it is important to perform matrix scans and compare the projected positions at the XBPM using the RFBPM and the position measured with the XBPM. Figure 4 shows a severe coupling problem of the vertical XBPM readings with the horizontal beam position. In this case it was caused by a 60-μm misalignment of the sensors on the left of the XBPM with those on the right: When the

beam is on one side horizontally, signals from only one pair of the diodes dominate and the vertical position reading is determined by their electric centerline. An offset is generated in Fig. 4 if the electric centerlines of the left and right diode pairs are at different heights. Similar problems have also been observed in conventional XBPMs where the two groups of blades are not symmetric due to assembly errors or physically damaged blades. When the offset is large, this asymmetry needs to be repaired. When the offset is small however, a compensation algorithm can be applied: we substitute the difference and sum in Eq. (1) with weighted versions defined as,

$$\begin{bmatrix} \Delta_x \\ \Sigma_x \\ \Delta_y \\ \Sigma_y \end{bmatrix} = \begin{bmatrix} a_{0x} & b_{0x} & c_{0x} & d_{0x} \\ a_{1x} & b_{1x} & c_{1x} & d_{1x} \\ a_{0y} & b_{0y} & c_{0y} & d_{0y} \\ a_{1y} & b_{1y} & c_{1y} & d_{1y} \end{bmatrix} \begin{bmatrix} A \\ B \\ C \\ D \end{bmatrix} - \begin{bmatrix} g_{0x} \\ g_{1x} \\ g_{0y} \\ g_{1y} \end{bmatrix} \quad (2)$$

and adjust the matrix elements so the XBPM readings from Eq. (1) coincide with the RFBPM projections at the XBPM location. It can be shown that this procedure can also fix other minor asymmetry problems caused by differences in PIN diodes and in amplifier gains. The lower panel of Figure 4 shows a sample data after the correction is applied to the raw data shown above.
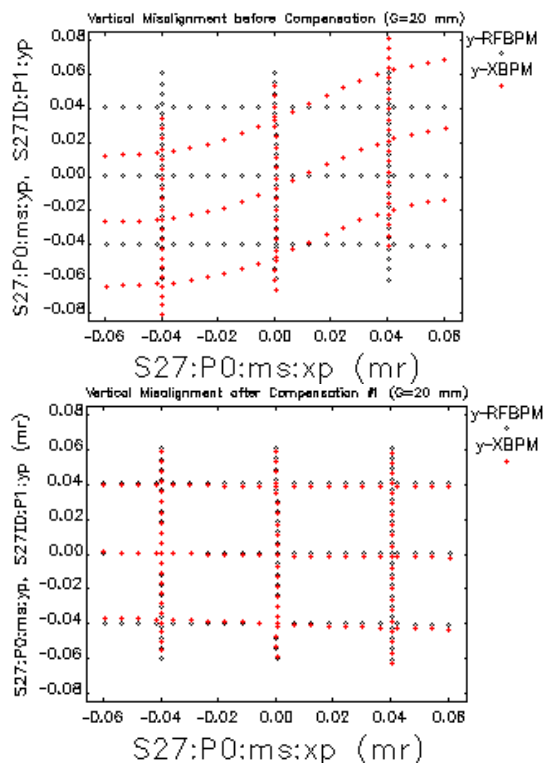

Figure 4: Top panel: The difference of projected electron beam vertical position (black) and the XBPM vertical position readings (red) in matrix scans show alignment errors in the XBPM components. Bottom panel: Compensation algorithm may be used to partially correct the asymmetry of the XBPM components.

Finally, if the horizontal steering range is small and each diode pair always has signals, the coupling problem can be avoided completely by using only one pair of diodes. Obviously, if any significant correction is applied at this step, the vertical and horizontal calibration will have to be repeated with the new matrix in Eq. (2).

SUMMARY AND DISCUSSIONS

A GRID-XBPM was installed in the APS high heat load front ends and was fully characterized. As a hard x-ray BPM, it demonstrated a 30-fold improvement in signal to BM background ratio over the old XBPM, which are sensitive to soft x-rays. Its vertical calibration is independent of gaps and remains unchanged for two different undulators. Its horizontal calibration changes with the undulator gap in a reproducible pattern, which can be interpolated with a simple expression. This type of XBPM should greatly improve the DC stability of the undulator beam since it directly measures the undulator white beam position and is insensitive to the BM background. Work is underway to incorporate the XBPM in the orbit control system for daily operations.

REFERENCES

[1] M. Borland et al., *these proceedings*, TUPJE063, IPAC'15, Richmond, VA (2015).

[2] N. S. Sereno et al., *these proceedings*, MOPW011, IPAC'15, Richmond, VA (2015).

[3] B. X. Yang, G. Decker, S. H. Lee, and P. Den Hartog, Proc. of BIW0210, Santa Fe, NM, p. 233, (2010), http://www.JACoW.org

[4] B.X. Yang, G. Decker, S. H. Lee, P. Den Hartog, T.-L. Kruy, J. Collins, M. Ramanathan, and N. G. Kujala, Proc. of BIW2012, Newport News, VA, p. 235, (2012), http://www.JACoW.org

[5] B.X. Yang, G. Decker, J. Downey, Y. Jaski, T. Kruy, S. H. Lee, M. Ramanathan and F. Westferro, Proc. of NAPAC 2013, Pasadena, CA, p. 1079, (2013), http://www.JACoW.org